Estimation of Source Parameters of Mega-Fault Systems for Strong Ground Motion Prediction
-Test Case: Arima-Takatsuki Fault Zone-

Shinichi Matsushima[1]

[1] *Deputy General Manager, Research Department, Ohsaki Research Institute, Tokyo, Japan*
Email: matsu@ohsaki.co.jp

ABSTRACT :
Predicting strong ground motion by earthquakes occurring on crustal mega-fault systems is crucial when we need to consider low occurrence-rate strong ground motion for seismic design of buildings. In order to predict strong ground motion by earthquakes occurring on inland crustal mega-fault systems, we need to estimate fault parameters for earthquakes of this kind. Since instrumental recording started in Japan, we have not encountered any inland crustal earthquakes that exceed magnitude 8. The source parameters of a mega-fault system from recorded earthquakes on the same fault system are estimated. The Headquarters for Earthquake Research Promotion (HERP) of Japan has evaluated several inland crustal mega-fault systems that will exceed magnitude 8 in Japan. For a test case the Arima-Takatsuki fault zone that extends about 130 km is considered. Source parameters of the Keicho-Fushimi earthquake of 1596, that ruptured the whole mega-fault system of the Arima-Takatsuki fault zone is estimated. Source parameters of the Hyogoken Nanbu (Kobe) earthquake of 1995 that occurred on the south-western portion of the same fault system have been estimated by Matsushima and Kawase (2006). Source parameters of the two earthquakes are compared, and the distribution of the stress drop seems to resemble each other. Although his result needs further investigation, it may be an indication that it can be used to estimate parameters for future earthquakes of mega-fault system from smaller earthquakes occurring on the same fault system.

KEYWORDS:
mega-fault system, strong ground motion, source parameter, Kobe earthquake, Keicho-Fushimi earthquake

1. INTRODUCTION

Predicting strong ground motion by earthquakes occurring on crustal mega-fault systems is crucial when we need to consider low occurrence-rate strong ground motion for seismic design of buildings. In order to predict strong ground motion by earthquakes occurring on inland crustal mega-fault systems, we need to estimate source parameters for earthquakes of this kind. Since instrumental recording started in Japan, we have not encountered any inland crustal earthquakes that exceed JMA magnitude 8. The Headquarters for Earthquake Research and Promotion (HERP) has evaluated several inland crustal mega-fault systems that will exceed magnitude 8 in Japan. For a test case, the Arima-Takatsuki fault zone, i.e. one of the evaluated mega-fault systems by HERP, will be considered in this study.
Source parameters of the Keicho-Fushimi earthquake of 1596, that is said to have ruptured the whole mega-fault system of the Arima-Takatsuki fault zone that extends nearly 130 km, are estimated. Since the earthquake occurred in the late 1500s, the information of the strong ground shaking is available only from limited explanations in written articles of the damage. Usami (2003) has compiled the information and estimated the seismic intensity. The seismic intensity will be used for target when I estimate the source parameters for this earthquake. As for the Hyogoken Nanbu (Kobe) earthquake of 1995 that is said to have occurred on one portion of the fault system, Matsushima and Kawase (2006) used several near-fault recordings to estimate the source parameters.
The source parameters of these two earthquakes are compared to find the difference between the estimated parameters, so that it can be used to estimate parameters for future earthquakes occurring on a mega-fault system from smaller earthquakes occurring on the same fault system.

2. THE 1596 KEICHO-FUSHIMI EARTHQUAKE

The 1596 Keicho-Fushimi (K-F) earthquake is assumed that to have occurred on the Arima-Takatsuki (A-T) fault zone that extends nearly 130km. Figure 1 shows the map of the region of interest and the six main faults of the A-T fault zone that is assumed to have slipped during the K-F earthquake.

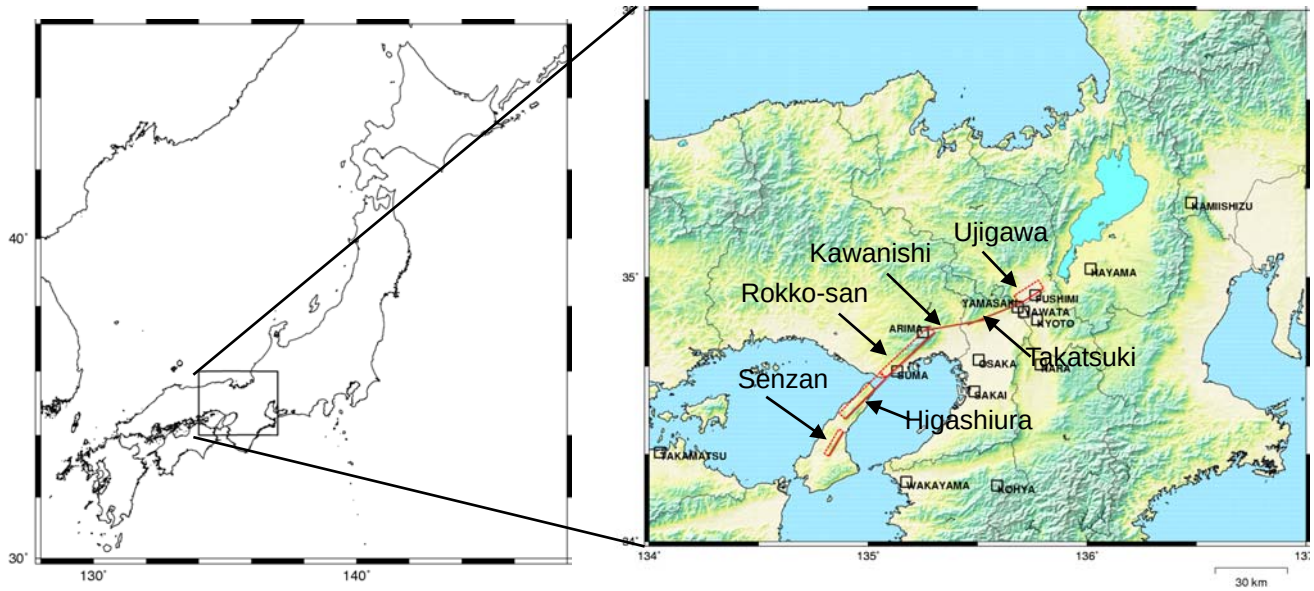

(a) Region of interest (b) Six main faults of the Arima-Takatsuki fault zone

Figure 1 Map of Japan and the Arima-Takatsuki fault zone.

Table 1 shows the parameters of each fault segment of the A-T fault zone. The fault segments of the shaded rows are the six main faults that are used in this study. The information of the surface faulting in only used to estimate the source parameters. To estimate the source parameters of the K-F earthquake, the maximum surface displacement is assumed to scale with the surface length of each fault segment. Table 2 shows the maximum surface displacement (D_{max}) that is derived from the surface length of each segment (L_{seg}) and average slip of the fault area (D_{ave}) that is derived from D_{max} together with the seismic moment (M_0). The relations of L_{seg} [km], D_{max} [m], D_{ave} [m], and M_0 [Nm],.

$$D_{max} = 0.18\, L_{seg} \tag{1}$$

$$D_{ave} = D_{max}\,/1.5/2.0 \tag{2}$$

$$M_0 = \mu\, L_{seg}\, W\, D_{ave} \tag{3}$$

are used. Here, μ [N/m^2] is rigidity of the media at the source depth and W.[km] is width of the fault segment. L_{seg} is calculated from the two ends of the fault described in Table 1. If L_{seg} is shorter than 20km, W is equal to L_{seg}. Otherwise, W is 20km. Figure 2 shows the relation between M_0 and S or D for the modeled Keicho-Fushimi earthquake. The relations are close to the Somerville *et al*. (1999) relations.

Table 3 shows the source parameters derived from the fault parameters in Table 2, using the so-called "Recipe for strong ground motion prediction" by Irikura and Miyake (2001). In this case, the depth of the upper rim of the fault model is assumed to be 3km. The total short-period level (A), i.e. flat level of the acceleration source spectrum, of the total fault is estimated from the empirical relations by Dan *et al*. (2001). The radius (r) of the total area of asperities is derived from the relation to A. The static stress drop ($\Delta\sigma_a$) of asperities is derived from M_0, r, and the radius of the total area of the fault (R). $\Delta\sigma_a$ is 15.3MPa for this fault model. The square of A and area of asperity is distributed proportional to the ratio of area of each segment.

Table 1 Segments of the Arima-Takatsuki fault zone
(Fault segments of shaded rows are the main six faults that is used in this study)

segment no.	name	length km	north-eastern end N DD	north-eastern end N MM	north-eastern end E DDD	north-eastern end E MM	south-western end N DD	south-western end N MM	south-western end E DDD	south-western end E MM	fault area dip deg.	fault area dip direc.	fault area bottom depth km
176-01	Ujigawa	15	34	57.0	135	48.5	34	53.5	135	42.0	70	N	15.0
176-02	Takatsuki	25	34	54.5	135	42.5	34	49.5	135	27.5	90	V	15.0
176-03	Baba	8	34	54.0	135	35.5	34	51.5	135	32.0	90	V	15.0
176-04	Minou	10	34	54.0	135	33.0	34	50.0	135	28.5	60	E	15.0
176-05	Satsukiyama	12	34	55.0	135	30.0	34	49.5	135	26.0	60	E	15.0
176-06	Itami	14	34	49.5	135	30.5	34	46.5	135	22.5	90	V	15.0
176-07	Rokko-san	27	34	47.5	135	18.5	34	37.0	135	5.0	80	N	15.0
176-08	Higashiura	26	34	37.0	135	5.0	34	28.0	134	54.0	80	W	15.0
176-09	Hokudan	21	34	37.0	135	4.5	34	31.5	134	54.0	90	V	15.0
176-10	Nishinomiya	21	34	46.5	135	21.5	34	41.0	135	10.5	60	N	15.0
176-11	Kawanishi	25	34	50.5	135	32.0	34	48.0	135	15.5	90	V	15.0
-	Senzan	12	34	25.0	134	53.5	34	19.5	134	49.5	80	W	15.0

Table 2 Fault parameters of the assumed fault model of the 1596 Keicho-Fushimi earthquake

Segment	Segment Length L_{seg} km	Maximum Displacement $D_{max}=0.18L_{seg}$ m	Average Slip of Fault Area $D_{ave}=D_{max}/1.5/2.0$ m	Width W km	Area $S=L\cdot W$ km^2	Seismic Moment M_0 N·m
Ujigawa	12	2.16	0.72	12	144	3.43E+18
Takatsuki	25	4.50	1.50	20	500	2.48E+19
Kawanishi	26	4.68	1.56	20	520	2.68E+19
Rokko-san	28	5.04	1.68	20	560	3.11E+19
Higashiura	24	4.32	1.44	20	480	2.29E+19
Senzan	12	2.16	0.72	12	144	3.43E+18
Total	127	5.04	1.4		2,348	1.12E+20

$\mu = 3.31 \times 10^{10}$ [N/m^2]

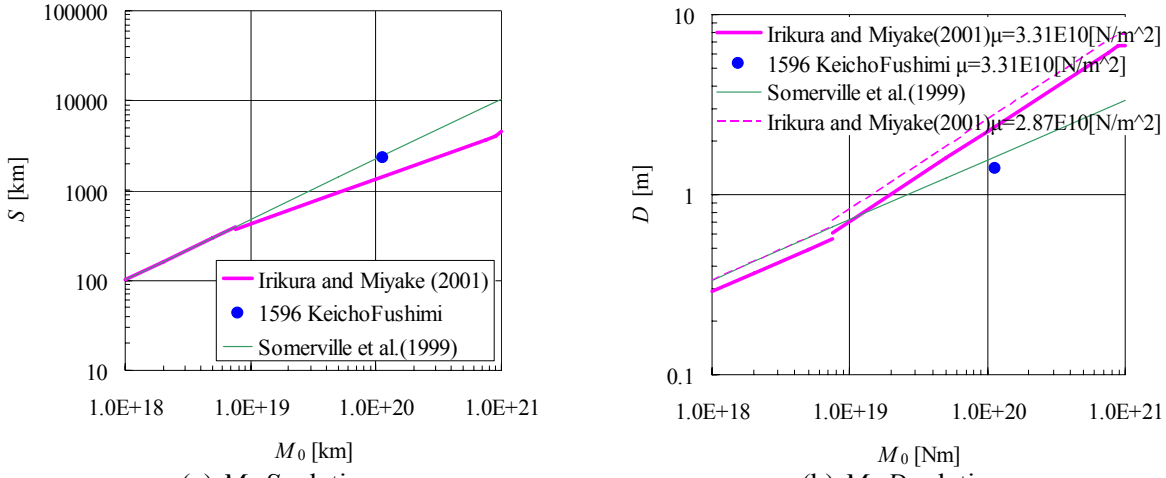

(a) M_0-S relation (b) M_0-D relation

Figure 2 M_0-S and M_0-D relation of the modeled Keicho-Fushimi earthquake compared with Irikura and Miyake (2001) and Somerville et al. (1999).

Table 3 Source parameters of the assumed 1596 Keicho-Fushimi earthquake

Parameters		Formula	1596 Keicho-Fushimi Earthquake					
			Ujigawa	Takatsuki	Kawanishi	Rokko-san	Higashiura	Senzan
Origin			34°57.0′ N 135°48.5′ E	34°54.5′ N 135°42.5′ E	34°50.5′ N 135°32.0′ E	34°47.5′ N 135°18.5′ E	34°37.0′ N 135°5.0′ E	34°25.0′ N 134°53.5′ E
Strike			N237E	N248E	N260E	N227E	N225E	N211E
Dip			70 °	90 °	90 °	80 °	80 °	80 °
Rake		right lateral slip	−180 °	−180 °	−180 °	−180 °	−180 °	−180 °
Length			12.0 km	25.0 km	26.0 km	28.0 km	24.0 km	12.0 km
Width		W=L (L<20km), W=20 (L>=20km)	12.0 km	20.0 km	20.0 km	20.0 km	20.0 km	12.0 km
Area		$S=L\cdot W$	144.0 km^2	500.0 km^2	520.0 km^2	560.0 km^2	480.0 km^2	144.0 km^2
Total Area		$S=\Sigma S_i$	2348 km^2					
Total Seismic Moment		$M_0=\Sigma M_{0i}$	1.12E+20 Nm					
Moment Magnitude		$M_w=(\log M_0(\mathrm{Nm})-9.1)/1.5$	7.3					
(JMA Magnitude)		$(M_J=(\log L+2.9)/0.6)$	(8.3)					
Average slip		$D=M_0/(\mu S)$	1.4 m					
Total Short Period Level		$A=2.46*10^{17}*M_0^{1/3}$[dyne cm]	2.56E+19 Nm/s^2					
Total Area of Asperities		$S_{asp}=\pi r^2$ $r=\frac{7\pi}{4}\frac{M_0}{AR}\beta^2$	368.5 km^2					
Total Static Stress Drop of Asperity		$\Delta\sigma_{asp}=7/16*M_0/(r^2R)$	15.3 MPa					
Segment	depth of top rim of fault		3.0 km	3.0 km	3.0 km	3.0 km	3.0 km	3.0 km
	Initiation Point	depends on hypocenter						
	Rupture Propagation		radial	radial	radial	radial	radial	radial
	Seismic Moment	$M_{0i}=\mu S_i D_i$	3.43E+18 Nm	2.48E+19 Nm	2.68E+19 Nm	3.11E+19 Nm	2.29E+19 Nm	3.43E+18 Nm
	Moment Magnitude	$M_w=(\log M_0(\mathrm{Nm})-9.1)/1.5$	6.3	6.9	6.9	6.9	6.8	6.3
	Average Slip	$D=M_0/(\mu S)$	0.7 m	1.5 m	1.6 m	1.7 m	1.4 m	0.7 m
	Rigidity	$\mu=\rho\beta^2,\rho=2.7g/cm^3,\beta=3.5km/s$	3.31E+10 N/m^2	3.31E+10 N/m^2	3.31E+10 N/m^2	3.31E+10 N/m^2	3.31E+10 N/m^2	3.31E+10 N/m^2
	S-wave Velocity	β=3.5km/s	3.5 km/s	3.5 km/s	3.5 km/s	3.5 km/s	3.5 km/s	3.5 km/s
	Rupture Velocity	$V_R=0.72*\beta$ km/s (Geller, 1976)	2.5 km/s	2.5 km/s	2.5 km/s	2.5 km/s	2.5 km/s	2.5 km/s
	Short-Period Level	Square of Short-Period Range proportional to ratio of area of segments	6.34E+18 Nm/s^2	1.18E+19 Nm/s^2	1.20E+19 Nm/s^2	1.25E+19 Nm/s^2	1.16E+19 Nm/s^2	6.34E+18 Nm/s^2
Total Asperity	Area	Proportional to ratio of area of segments	22.6 km^2	78.5 km^2	81.6 km^2	87.9 km^2	75.3 km^2	22.6 km^2
	Average Slip	$D_a=\gamma_D\cdot D$	1.4 m	3.0 m	3.1 m	3.4 m	2.9 m	1.4 m
	Seismic Moment	$M_{0a}=\mu S_a D_a$	1.08E+18 Nm	7.79E+18 Nm	8.37E+18 Nm	9.88E+18 Nm	7.17E+18 Nm	1.08E+18 Nm
	Static Stress Drop	$\Delta\sigma_{asp}=7/16*M_0/(r^2R)$	15.3 MPa	15.3 MPa	15.3 MPa	15.3 MPa	15.3 MPa	15.3 MPa
First Asperity	Area	2/3 of total asperity	22.6 km^2	52.3 km^2	54.4 km^2	58.6 km^2	50.2 km^2	22.6 km^2
	Average Slip	$M_{0a1}=\mu S_{a1} D_{a1}$	1.4 m	3.3 m	3.4 m	3.8 m	3.2 m	1.4 m
	Seismic Moment	Proportional to power of 1.5 of asperity area	1.08E+18 Nm	5.75E+18 Nm	6.18E+18 Nm	7.30E+18 Nm	5.30E+18 Nm	1.08E+18 Nm
	Effective Stress	$\sigma_{asp}=\Delta\sigma_{asp}$	15.3 MPa	15.3 MPa	15.3 MPa	15.3 MPa	15.3 MPa	15.3 MPa
Second Asperity	Area	1/3 of total asperity		26.2 km^2	27.2 km^2	29.3 km^2	25.1 km^2	
	Average Slip	$M_{0a2}=\mu S_{a2} D_{a2}$		2.4 m	2.4 m	2.7 m	2.3 m	
	Seismic Moment	Proportional to power of 1.5 of asperity area		2.03E+18 Nm	2.19E+18 Nm	2.58E+18 Nm	1.87E+18 Nm	
	Effective Stress	$\sigma_{asp}=\Delta\sigma_{asp}$		15.3 MPa	15.3 MPa	15.3 MPa	15.3 MPa	
Backgroud	Seismic Moment	$M_{0b}=M_0-M_{0asp}$	2.35E+18 Nm	1.70E+19 Nm	1.85E+19 Nm	2.12E+19 Nm	1.57E+19 Nm	2.35E+18 Nm
	Area	$S_b=S-S_{asp}$	121.4 km^2	421.5 km^2	438.4 km^2	472.1 km^2	404.7 km^2	121.4 km^2
	Average Slip	$D_b=M_{0b}/(\mu S_b)$	0.6 m	1.2 m	1.3 m	1.4 m	1.2 m	0.6 m
	Effective Stress	$\sigma_b=(D_b/W_b)/(D_{asp}/W_{asp})*\Sigma S_{ai}^3/S_a^3*\sigma_{asp}$	2.5 MPa	2.0 MPa	2.1 MPa	2.1 MPa	2.0 MPa	2.5 MPa

The seismic intensity is calculated based on statistical Green's function method (Fujikawa *et al.*, 2003). First, the ground motion at the top of the engineering bedrock (V_s = 0.4 km/s, ρ = 1750 kg/m^3) is calculated considering the impedance contrast from the seismic bedrock (V_s = 3.5 km/s, ρ = 2700 kg/m^3). The frequency dependence of the radiation pattern characteristic is considered. The radiation pattern coefficient changes linearly from 2 to 6 Hz. For frequencies larger than 6 Hz, the radiation pattern is set to be isotropic. The Q value

dependent of the frequency, Q=37 $f^{0.84}$ and f_{max} 6 Hz is assumed. The velocity amplification between the engineering bedrock and the surface is estimated from the geomorphologic classification distributed by HERP. The same methodology HERP (2007) uses for making the hazard map is used to estimate the seismic intensity at the surface. The velocity amplification factor from engineering bedrock to surface is shown in Figure 3.
I considered twelve different patterns of distribution of asperities and initiation points and simulated the seismic intensity at 14 locations that the seismic intensity is known. The locations are plotted in Figure 1 with squares. The simulated intensity is compared with the observed intensity to find the best-fit model. Figure 4 shows the distribution of seismic intensity compared to the observed ones at the 14 locations colored with the observed intensity. The best-fit model is illustrated in Figure 5.

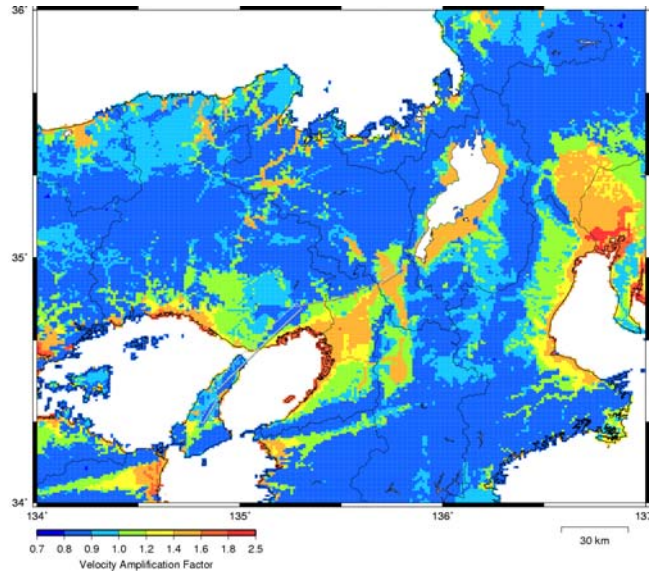

Figure 3 Velocity amplification factor from engineering bedrock to surface

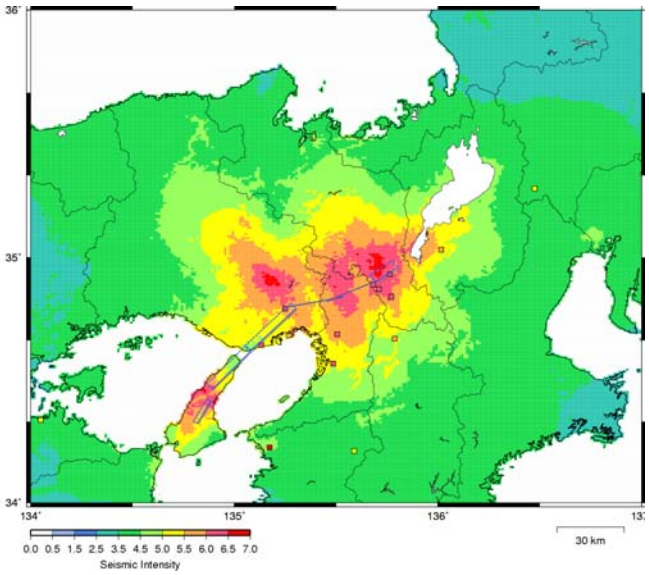

Figure 4 Seismic intensity distribution (Colored squares are the observed intensity)

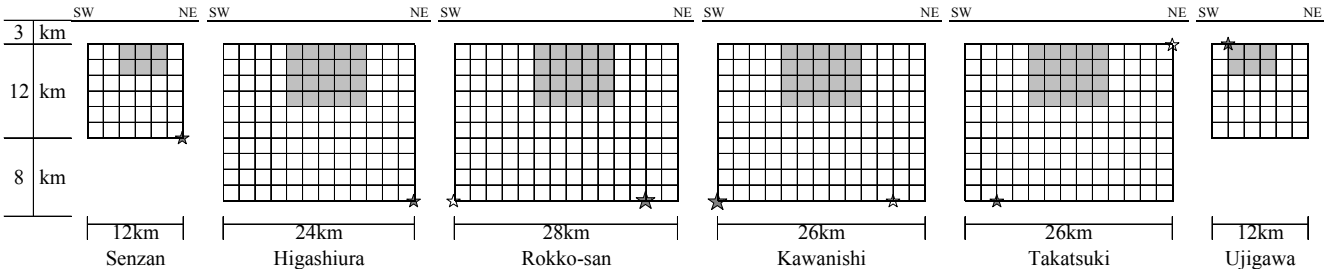

Figure 5 Asperity and initiation distribution of fault model of the best-fit case

3. THE 1995 HYOGO-KEN NANBU (KOBE) EARTHQUAKE

The heterogeneous rupture process of the 1995 Kobe earthquake had been determined by Kawase *et al*. (2000). They determined a four strong-motion-generation-area (SMGA) model that simulates the deconvolved bedrock motion at Kobe observatory of the Japan Meteorological Agency (JMA) and also explains time differences of pulses at Kobe University station by CEORKA (KBU) and Motoyama First Elementary School station by CEORKA (MOT). They combined this rupture model with a 3-D basin structure and simulated the strong ground motion in the Kobe area. As a result, they were successful in reproducing the “disaster-belt” that was formed along the strike of the Rokko faults, in the eastern part of Kobe. Unfortunately, they were not so successful in simulating the large velocity pulse that was recorded at JR Takatori station by JR (TKT) and the “disaster-belt” in the western region.
Matsushima and Kawase (2006) have re-evaluated the rupture process of the Kobe earthquake in order to get a model that can explain the recorded velocity pulse at TKT. First, they calculated 3-D Green’s function by finite difference method by Graves (1996). The 3-D velocity model they used was tuned-up using aftershock

recordings by Matsushima *et al*. (2000). They used the 3-D Green's function to find a best-fit combination of parameters by grid-search method. They assumed 9 parameters to search. Origin of SMGA (X0, Y0), size of SMGA (L, W), characteristics of the slip velocity time function in each SMGA (maximum velocity: Vd, time of maximum velocity: td, duration: tr, factor of shape function: α, and rake angle: λ). The rupture velocity was set to 2.8 km/s (80% of shear wave velocity). Figure 6 shows the region of the fault region to search, together with the area of the 3-D velocity model and the location of four stations used as targets. The target in their grid-search analysis was the N33W component (fault normal component) of the velocity waveform low-pass filtered at 2.5 Hz, at the four stations in Figure 6.
Figure 7 shows the fit between the observed (red) and synthetics of the best-fit case (blue). Figure 8 shows the evaluated slip velocity time functions, location and size of SMGAs. The fifth SMGA is assumed in the shallow part of third SMGA in order to fit the large velocity pulse at TKT. The initiation point for the first four SMGAs is the lower SW corner, but for the fifth SMGA, the initiation point is at the lower NE corner. This is because the large pulse at TKT moves toward the N147E direction while other pulses move toward the N33E direction.

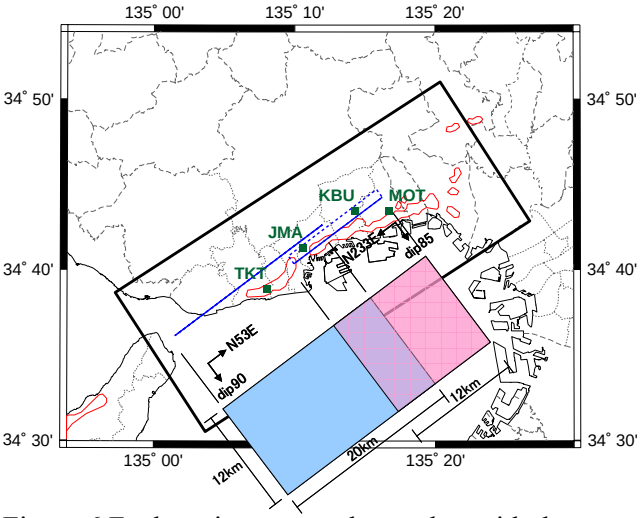

Figure 6 Fault region to search together with the area of 3-D velocity model and target stations
(dip angle blue plane is 90 de. and pink plane is 85 deg.)
(After Matsushima and Kawase (2006))

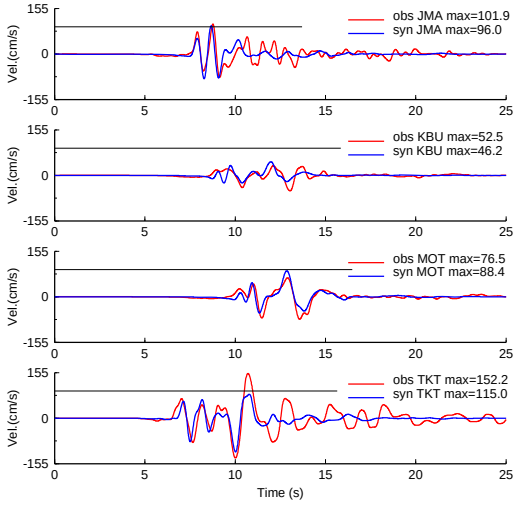

Figure 7 Comparison of the velocity waveforms of the observed (red) and synthetics of best-fit case (blue) at the four target stations (f < 2.5Hz)
(After Matsushima and Kawase (2006))

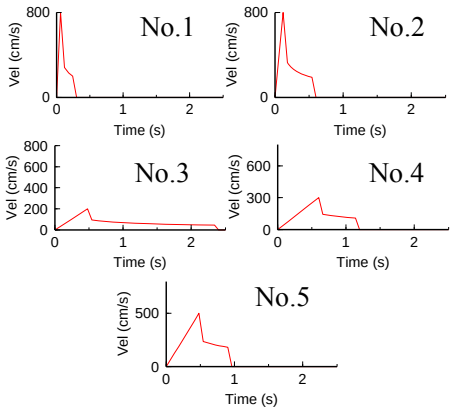

(a) Slip velocity time function of each SMGA

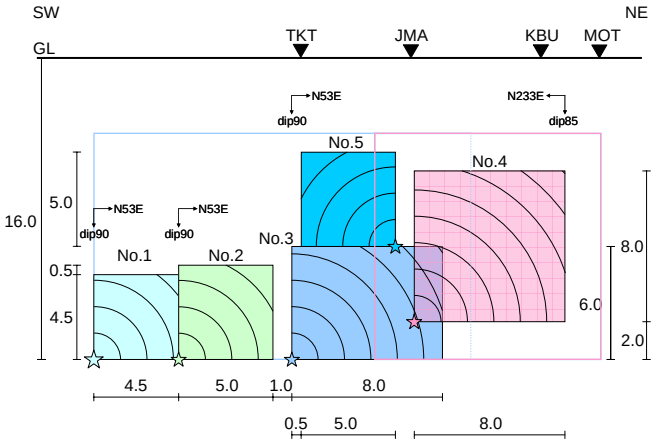

(b) Location and size of SMGA

Figure 8 Slip velocity time function, location and size of the SMGA (After Matsushima and Kawase (2006))

The source parameters of the best-fit case are listed in Table 4. The static stress drop $\Delta\sigma$ [MPa] is estimated from the evaluated parameters using the formulation derived from dynamic source simulation by Nakamura and Miyatake (2000),

$$V_m = \Delta\sigma\sqrt{2 f_c W V_R}\,/\,\mu \qquad (4)$$

where V_m [m/s] is maximum slip velocity function, f_c is corner frequency ($\sim f_{max}$), W [km] is the width of SMGA, V_R [km/s] is rupture velocity, and μ [N/m^2] is rigidity.
They simulated the PGV distribution considering the re-evaluated rupture process. The area of PGV 100cm/s and greater fits the region of the JMA seismic intensity 7 fairly well in the western part of Kobe, as well as the eastern part.

Table 4 Re-evaluated source parameter of SMGA for the Kobe earthquake

No.	M_0 x 10^{18} [Nm]	size L x W [km] [km]	start of rupture [sec]	total slip [m]	max. slip velocity time func. [cm/s]	static stress drop [MPa]
1	0.61	4.5 4.5	0.00	0.91	800	21.0
2	1.43	5.0 5.0	1.61	1.74	800	20.0
3	2.61	8.0 6.0	3.75	1.68	200	4.6
4	3.43	8.0 8.0	6.10	1.66	300	5.9
5	1.82	5.0 5.0	4.94	2.22	500	12.5
total	9.90	area=182 km^2				

4. COMPARISON OF THE SOURCE PARAMTERS

Figure 11 shows the comparison of the slip distribution between the Rokko-san segment of the 1596 Keicho-Fushimi earthquake and the Kobe segment of the 1995 Kobe earthquake. In the Kobe earthquake, the Awaji segment (Hokudan fault) had surface faulting, but it is not studied because of lack of near fault recordings. The fault that ruptured in Awaji Island in the Keicho-Fushimi earthquake is said to be the Higashiura and Senzan faults and not the Hokudan fault. Although we assumed a different dip angle in the analysis for the two different earthquakes, we assume that it is same for both earthquakes at this segment when we compare the two. The asperity of the K-F earthquake is surrounded by the first four SMGA of the Kobe earthquake. The fifth SMGA is located within the asperity. The static stress drop estimated for the fifth SMGA is about 12.5 MPa and it is twice as large as the third and fourth SMGA. The static stress drop estimated from the “recipe” for the asperities for K-F earthquake is estimated about 15.3 MPa and 2.1 MPa for the surrounding fault.

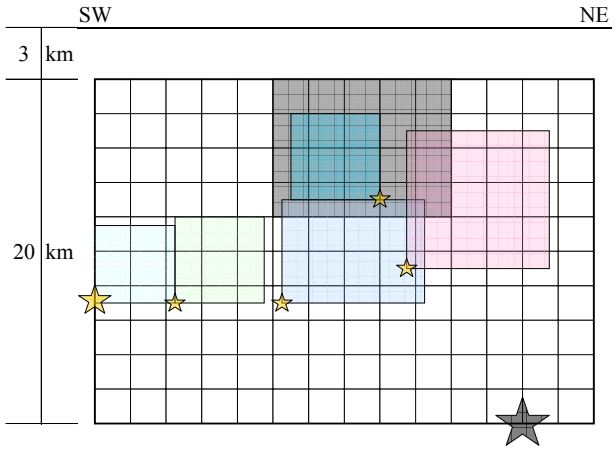

Figure 11 Comparison of the estimated slip distribution between Rokko-san segment of the K-F earthquake (hatched in gray) and Kobe segment of the Kobe earthquake (hatched by colors).
(The largest star and smaller stars denotes the initiation point for the K-F earthquake and the Kobe earthquake, respectively)

5. CONCLUSION

The source parameters for two earthquakes occurring on the same mega-fault system, one that ruptured the whole fault system and one that rupture only one portion of the fault system, were estimated. The pattern of the distribution of the stress drop seems to resemble each other, yet the absolute amount needs further investigation. This result may indicate that the static stress drop depends on the medium at the fault, meaning that it may be possible to predict the stress drop at a certain area of a fault of future earthquakes. The stress drop of the first and second SMGA is larger than the fifth SMGA and the asperity. The correspondence of these SMGA with the asperity also needs further investigation.
This is only one case that is studied. Also there is still concern about the evaluation of the source parameters of the K-F earthquake, since the seismic intensity at several locations are not reproduced well. So, there is need for further studies to confirm the hypothesis from this study.

ACKNOWLEDGEMENTS

Part of this study was supported by the JNES research topic (P.I.: K. Irikura) of the 2006 fiscal year. Discussions with co-researchers, Drs Kojiro Irikura, Yasuo Awata, Takao Kagawa, Ken Miyakoshi, Hiroe Miyake, Kazuo Dan, and Toshiaki Sato had been illuminating. Most of the figures were prepared using GMT software (Wessel and Smith, 1998).

REFERENCES

Fujikawa, S., Hayakawa, T., Watanabe, M., Matsushima, S., Sato, T., Dan, K., Fukuwa, N. and Kubo, T. (2003). Site-Specific Strong Motion Prediction in Nagoya Region, Central Japan Part 1: Strong Motion Simulation for An Anticipated Tokai Earthquake. *Summaries of Technical Papers of the Annual Meeting Architectural Institute of Japan*. **B-2**, 155-156 (in Japanese).
Graves, R.W. (1996). Simulation Seismic Wave Propagation in 3D Elastic Media Using Staggered-Grid Finite Differences. *Bulletin of Seismological Society of America* **86:4**, 1091-1101.
Irikura, K. and Miyake, H. (2001). Prediction of strong ground motions for scenario earthquakes. *Journal of Geography* **110**, 849-875 (in Japanese with English abstract).
Kawase, H., Matsushima, S., Graves, R.W. and Somerville, P.G. (2000). Strong motion simulation of Hyogo-ken Nanbu (Kobe) earthquake considering both the heterogeneous rupture process and the 3-D basin structure. *Proceedings of the 12th World Conference on Earthquake Engineering* Auckland, New Zealand, CD-ROM Ref. 990, pp.8.
Matsushima S. and Kawase H. (2006). Re-Evaluation of Near Source Strong Ground Motion During the 1995 Kobe Earthquake Considering The Heterogeneity of Source and 3-D Basin. *Proceedings of the Third International Symposium on the Effects of Surface Geology on Seismic Motion, Grenoble, France* 141, 617-625.
Somerville, P., Irikura, K., Graves, R., Sawada, S., Wald, D., Abrahamson, N., Iwasaki, Y., Kagawa, T., Smith, N. and Kowada, A. (1999). Characterizing earthquake slip models for the prediction of strong ground motion. *Seismological Research Letters* **70**, 59-80.
The Headquarters for Earthquake Research Promotion. (2007). National Seismic Hazard Maps for Japan, 2006.
Usami, T. (2003). Conspectus of Damage Earthquakes in Japan [416]-2001, University of Tokyo Press, pp.605 (in Japanese).
Wessel, P. and Smith, W.H.F. (1998). New, improved version of Generic Mapping Tools released, *EOS Transactions of AGU* **79:47**, pp.579.